Kinematical structure of open clusters within 1 kpc by Gaia

W. H. Elsanhoury[1,2]

[1] Astronomy Department, National Research Institute of Astronomy and Geophysics (NRIAG), 11421, Helwan, Cairo, Egypt (Affiliation ID: 60030681)

[2] Physics Department, Faculty of Science and Arts, Northern Border University, Rafha Branch, Saudi Arabia

welsanhoury@gmail.com

(Submitted on 07.05.2019. Accepted on 22.06.2019)

Abstract. The work is based on proper motions, radial velocities, and absolute magnitudes of 56 open clusters located within 1 kpc. We classify those as a function of their distances into five groups (Freedman and Diaconis's rule) as well as a double frequency table may be achieved. For these groups, we calculated their velocity ellipsoid parameters VEPs, e.g. space velocity, dispersion velocity, elements of the Solar motion, and dispersion ratio (σ_2/σ_1).

For the first group of these open clusters with distances $98.717 \leq r \leq 310.078$ pc, the dispersion ratio is in the range of 0.65-0.74, which is in a good agreement with that deduced by Oort. Finally, we have determined their luminosity and mass functions.

Key words: Open clusters within 1 kpc – Gaia DR2 – Velocity Ellipsoid Parameters VEPs – Oort's constants – Luminosity and mass functions.

Introduction

Star clusters are the main building blocks of the stellar populations in our Galaxy (Kharchenko et al., 2013), these groups of stars are formed from the same molecular cloud and have roughly the same age, distance, chemical composition, and are visible up to large distances. Since open clusters are distributed throughout the Galactic disc and span a wide range in age, they are a very useful tool for studying and estimating the effects of the dynamical evolution of the Galactic disc and trace the spiral arms (Joshi et al., 2016).

Open clusters are convenient probes of the structure and history of the Galactic disc. They are also fundamental to stellar evolution studies. The second Gaia data DR2 [3] (Cantat-Gaudin et al., 2018) release contains precise astrometry at the sub-milliarcsecond level and homogeneous photometry at the mmag level, that can be used to characterize a large number of clusters over the entire sky (Cantat-Gaudin et al., 2018). Gaia DR2 provides high-precision astrometry and three-band photometry (G, G_{BP}, and G_{RP}) for about 1.3 billion sources over the full sky.

The precision, accuracy, and homogeneity of both astrometry and photometry are unprecedented. Proper motions could be used to estimate membership probabilities and to select the most probable cluster members. Nearby open clusters within 1 kpc can provide more precise determination of their kinematical structure, like equatorial coordinates of the vertex, that is its right ascension and declination (A_o, D_o) and analysis of their luminosity and mass functions (Elsanhoury et al., 2016).

[3] http://cdsarc.u-strasbg.fr (130.79.128.5) or via
http://cdsweb.u-strasbg.fr/cgi-bin/qcat?J/A+A/618/A93

The velocity distribution of the stream of stars in the nearby Solar neighborhood has been characterized as an ellipsoid, the centroid, size, and orientation of which vary systematically with the ages (and hence colors) of the stars under investigations (Hogg et al., 2005 and Dehnen & Binney, 1998).

The structure of this article is as follows: Sec. 1 presents the data sample. Sec. 2 is devoted to the kinematical structure. Sec. 3 presents the luminosity and mass functions analysis. Results and discussion are presented in Sec. 4. The conclusion is outlined in the final section.

1. Data sample

In this survey, open clusters of distances ($r \leq 1$ kpc) on the sky are the main targets selected only with known proper motion in both directions and parallaxes. In this context, we have extracted about 201 open clusters with the aid of Gaia DR2 source (Cantat-Gaudin et al., 2018).

The astrometric uncertainties in Gaia DR2 will be at the level of tens of micro-arcsec for sources $G < 15$, also it presents a complete photometric catalog of the sources on all-sky homogeneous photometric systems in the Gaia G band and broad bands G_{BP} & G_{RP}.

The data set used in the present work computations is presented by Gaia DR2 data including right ascension, declination, proper motions in both directions of right ascension & declination, and the distances. In what follows, we can analyze their kinematic and magnitude behavior (i.e. luminosity and mass functions).

For our purpose, Table 1 presents a final worksheet data sample (i.e. 56) of open clusters with only positive radial velocities ($V_r > 0$) criterion by Kharchenko et al. (2013). The columns are labeled as follows: the name of open cluster in column 1, the right ascension α_{2000}(deg) and declination δ_{2000}(deg) in columns 2 and 3 respectively, the distance (pc) in column 4, proper motions in both directions with their errors (mas/yr) in columns 5, 6, 7, and 8 respectively, the columns 9 and 10 give the radial velocity (km/s) with their errors respectively, column 11 present the absolute magnitude (mag) by Kharchenko et al. (2016), and finally column 12 gives the number of the group that cluster falls into.

According to Freedman & Diaconis (1981) rule, we can divide these 56 open clusters into five groups according to their distances. The steps in constructing a frequency distribution of these open clusters under consideration are as follows:
(i) The number k of intervals can be determined with,
k =[(max. distance - min. distance)/h] = (967.118 - 98.717)/h = 4.108.
where h is the bin width.
(ii) The bin width h, according to Freedman & Diaconis (1981) is, $h = 2\ IQR/\sqrt[3]{n} = 211.361$, where n is the sample size (i.e. 56), and IQR is the sample interquartile range.
(iii) The sample interquartile range $IQR = 404.3196$.

Figure 1 presents the Histogram plot of the distribution of these clusters per distance (pc) into five groups. Table 2 presents the intervals (classes),

into which first and second columns gives the group number and the center of the interval (an average of the lower and upper limits) respectively, and the last column gives the frequencies. Here, we may note that about 79% of the whole sample is concentrated in the first, second, and fourth intervals with corresponding frequencies of about 13, 19 and 12 respectively.

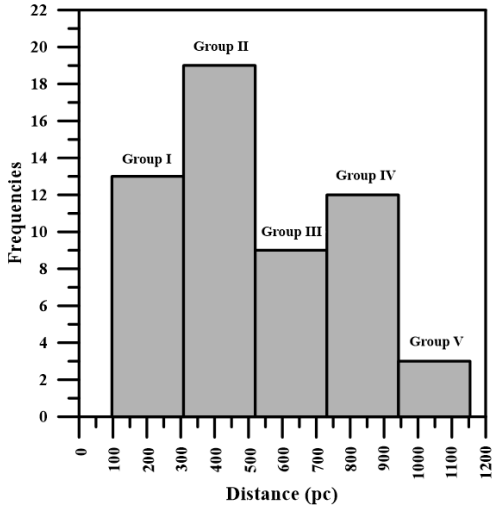

Fig. 1. Histogram distribution of 56 open clusters into five groups

2. Kinematical structure

According to well-known formulae (Smart, 1958), the expressions of components of space velocity (V_x, V_y, and V_z) along x, y, and z-axes of a coordinate system whose center is the Sun and such that the x-axis points towards the point ($\alpha = 0^h, \delta = 0^o$), the y-axis is oriented towards the point ($\alpha = 6^h, \delta = 0^o$) and the z-axis towards the north celestial pole at a definite epoch, are

$$V_x = -4.74 r \mu_\alpha cos\delta sin\alpha - 4.74 r \mu_\delta cos\alpha sin\delta + V_r cos\delta cos\alpha, \quad (1)$$

$$V_y = 4.74 r \mu_\alpha cos\delta cos\alpha - 4.74 r \mu_\delta sin\alpha sin\delta + V_r cos\delta sin\alpha, \quad (2)$$

$$V_z = 4.74 r \mu_\delta cos\delta + V_r sin\delta. \quad (3)$$

Now we compute the space velocity components U, V and W along the three axes with Liu et al. (2011) which used an equatorial Galactic

Table 1. Fundamental parameters of 56 open clusters within $r \leq 1$ kpc presented by Cantat-Gaudin et al. (2018), their radial velocities (Kharchenko et al., 2013), and absolute magnitudes (Kharchenko et al. 2016)

Cluster Name	Ra_{J2000} (deg.)	Dec_{J2000} (deg.)	r(pc)	μ_α(mas/yr)	$\sigma_{\mu\alpha}$(mas/yr)	μ_δ(mas/yr)	$\sigma_{\mu\delta}$(mas/yr)	V_r (km/s)	σ_{V_r}(km/s)	M_J	Group No.
Mamajek 1	130.637	-78.963	98.717	-29.834	1.81	26.99	1.212	15	1.05	-0.373	I
Alessi 13	51.762	-35.821	104.341	36.332	0.931	-4.709	0.851	19.5	3	-0.252	I
Platais 8	136.718	-58.685	134.862	-15.596	1.26	14.474	1.164	17.3	3.09	-2.507	I
IC 2391	130.292	-52.991	151.930	-24.644	0.883	23.316	0.733	14.6	1.39	-2.343	I
IC 2602	160.613	-64.426	152.416	-17.582	0.833	10.7	0.902	21.9	2.54	-2.898	I
Platais 3	69.976	71.28	177.936	3.616	1.275	-20.931	0.626	7	3.7	-0.352	I
Platais 9	139.241	-43.862	183.050	-24.705	1.086	13.333	0.583	17.8	1.48	-2.113	I
NGC 2632	130.054	19.621	186.532	-36.09	1.115	-12.919	0.997	33.4	0.52	-3.317	I
NGC 2451A	115.736	-38.264	193.611	-21.116	0.853	15.328	0.708	22.6	4.49	-2.538	I
Blanco 1	0.853	-29.958	237.530	18.739	0.432	2.602	0.444	5.5	2.04	-1.945	I
Alessi 3	109.275	-46.142	280.426	-9.875	0.447	11.958	0.515	20	7.4	-1.75	I
Collinder 135	109.362	-37.044	305.064	-9.975	0.445	6.157	0.35	15.4	2.2	-2.838	I
Ruprecht 147	289.087	-16.333	307.692	-0.939	0.445	-26.576	0.581	41	-	-3.489	I
IC 348	56.132	32.159	324.781	4.483	0.593	-6.447	0.603	16	3.77	-1.686	II
NGC 2232	96.888	-4.749	326.052	-4.745	0.291	-1.84	0.252	19.8	4.54	-2.681	II
ASCC 21	82.179	3.527	348.918	1.404	0.263	-0.632	0.238	19.9	1.14	-3.23	II
ASCC 16	81.198	1.655	352.361	1.355	0.265	-0.015	0.248	30	-	-2.12	II
ASCC 19	81.982	-1.987	361.272	1.152	0.252	-1.234	0.219	19.8	3.17	-1.203	II
NGC 2451B	116.128	-37.954	367.782	-9.671	0.409	4.702	0.281	13.7	7.13	-7.89	II
Stock 2	33.856	59.522	378.645	15.966	0.65	-13.627	0.591	1.8	1.82	-5.027	II
Collinder 140	110.882	-31.966	385.505	-8.074	0.277	4.789	0.258	22.9	0.83	-1.894	II
NGC 2547	122.525	-49.198	391.696	-8.609	0.283	4.262	0.28	14.8	1.94	-2.505	II
Alessi 5	160.819	-61.081	399.840	-15.411	0.324	2.503	0.348	8.2	6.69	-2.574	II
Collinder 69	83.792	9.813	406.174	1.194	0.55	-2.118	0.393	31.4	1.42	-4.585	II
NGC 2516	119.527	-60.8	413.736	-4.748	0.441	11.221	0.345	21.2	1.08	-6.539	II
Turner 5	143.284	-36.358	421.408	0.092	0.248	-3.115	0.185	11.4	2.69	-2.589	II
Trumpler 10	131.943	-42.566	437.254	-12.532	0.401	6.527	0.275	15	15	-2.883	II
NGC 752	29.223	37.794	446.628	9.81	0.272	-11.713	0.266	4.7	0.75	-4.198	II
Alessi 10	301.233	-10.555	447.828	1.469	0.208	-7.879	0.241	75.9	2.6	-1.506	II
NGC 2422	114.147	-14.489	483.092	-7.057	0.259	0.993	0.247	36.7	2.92	-4.926	II
NGC 3532	166.417	-58.707	484.027	-10.385	0.396	5.175	0.404	1.2	0.72	-5.165	II
ASCC 58	153.657	-55.001	485.437	-13.276	0.21	2.786	0.271	8	3.7	-3.057	II
NGC 2281	102.091	41.06	527.426	-2.946	0.274	-8.321	0.257	13.3	4.11	-4.073	III
Haffner 13	115.209	-30.073	574.053	-6.184	0.26	5.879	0.193	68	5.8	-2.832	III
Alessi 21	107.69	-9.363	581.395	-5.475	0.194	2.602	0.162	38.8	1.8	-2.314	III
NGC 2527	121.246	-28.122	651.042	-5.549	0.229	7.275	0.212	39.6	0.1	-3.072	III
Collinder 132	108.485	-30.758	666.223	-4.14	0.193	3.732	0.148	28	3.7	-1.419	III
Pismis 4	128.79	-44.407	707.214	-8.236	0.166	5.337	0.145	27.2	0.92	-1.506	III
NGC 6716	283.616	-19.888	711.744	-1.476	0.199	-6.013	0.184	6	7.4	-2.759	III
Alessi 1	13.343	49.536	719.425	6.536	0.105	-6.245	0.204	6	1.8	-3	III
IC 2395	130.531	-48.09	725.163	-4.464	0.237	3.293	0.296	13.2	9.76	-3.998	III
NGC 2287	101.499	-20.716	735.294	-4.339	0.178	-1.381	0.199	24.5	1.2	-6.023	IV
NGC 2264	100.217	9.877	738.552	-1.69	0.508	-3.727	0.251	20.7	1.53	-4.413	IV
Loden 1194	212.006	-59.786	752.445	-7.762	0.171	-4.667	0.202	2	3.7	-1.431	IV
NGC 2925	143.321	-53.413	772.201	-8.533	0.171	5.336	0.145	16	7.4	-2.923	IV
NGC 2548	123.412	-5.726	775.795	-1.313	0.194	1.029	0.178	41.5	0.3	-4.941	IV
ASCC 79	229.731	-60.798	850.340	-2.914	0.375	-4.232	0.472	4.5	2.65	-6.043	IV
ASCC 11	53.056	44.856	876.424	0.926	0.163	-3.03	0.147	0.7	5.64	-5.845	IV
NGC 2301	102.943	0.465	881.057	-1.367	0.208	-2.179	0.187	39.6	12.35	-3.143	IV
NGC 2682	132.846	11.814	881.057	-10.986	0.193	-2.964	0.201	33.6	0.19	-5.025	IV
ASCC 85	251.853	-45.555	893.655	0.17	0.124	-4.102	0.138	7.1	-	-3.482	IV
Alessi 6	220.058	-66.127	909.091	-10.472	0.15	-5.559	0.163	9.2	1.16	-2.465	IV
Ruprecht 161	152.4	-61.259	920.810	-10.391	0.122	3.742	0.196	9.4	3.7	-2.501	IV
NGC 2423	114.299	-13.863	956.938	-0.735	0.124	-3.632	0.149	21.7	2.54	-3.943	V
Collinder 197	131.202	-41.28	967.118	-5.808	0.305	3.933	0.388	33.1	3.2	-2.546	V
NGC 2546	123.082	-37.661	967.118	-3.757	0.095	3.862	0.139	36	4.1	-4.996	V

Table 2. Frequency distribution of 56 open clusters under study

Group No.	Intervals (pc)	Center of interval	Frequencies
I	98.717 - 310.078	204.3975	13
II	310.078 - 521.439	415.7585	19
III	521.439 - 732.800	627.1195	9
IV	732.800 - 944.161	838.4805	12
V	944.161 - 1155.522	1049.8415	3
Sum			$\Sigma = 56$

transformation. They determine the position of the Galactic plane using recent catalogs like Two-Micron All-Sky Survey 2MASS and define the optimal Galactic coordinate system by adopting the ICRS position of the compact radio source Sagittarius A^*.
i.e.

$$U = -0.0518807421V_x - 0.8722226427V_y - 0.4863497200V_z, \quad (4)$$

$$V = 0.4846922369V_x - 0.4477920852V_y + 0.7513692061V_z, \quad (5)$$

$$W = -0.8731447899V_x - 0.1967483417V_y + 0.4459913295V_z. \quad (6)$$

While the mean velocities are calculated as:

$$\overline{U} = \frac{1}{N}\sum_{i=1}^{N} U_i, \quad (7)$$

$$\overline{V} = \frac{1}{N}\sum_{i=1}^{N} V_i, \quad (8)$$

$$\overline{W} = \frac{1}{N}\sum_{i=1}^{N} W_i. \quad (9)$$

To compute the parameters of the ellipsoidal velocities for the groups in Table 2, we used a computational algorithm presented by Elsanhoury et al. (2013) and Elsanhoury et al. (2015). The space velocities (U, V, W) and their average $(\overline{U}, \overline{V}, \overline{W})$ are computed.

In addition, the coordinates Q_i of the point i with respect to an arbitrary axis ξ centered on the stellar distribution's center are determined. Following, the above-mentioned algorithm, the generalized form of the mean square deviation σ^2, the direction cosines (l_i, m_i, n_i), from which a symmetric matrix with elements μ_{ij} and the eigenvalues $\lambda_{1,2,3}$ are calculated.

Now, we establish analytical expressions of the parameters in terms of the matrix elements μ_{ij} of the eigenvalue problem for the velocity ellipsoid

(i.e. Velocity Ellipsoid Parameters VEPs).
• *The* $\sigma_i; i = 1, 2, 3$ *parameters*
The dispersion velocity $\sigma_i; \forall i = 1, 2$ and 3 parameters are defined as

$$\sigma_i = \sqrt{\lambda_i} \tag{10}$$

• *The* (l_i, m_i, n_i) *parameters*
The direction cosines l, m, and n are mathematically represented as follows:

$$l_i = \left[\mu_{22}\mu_{33} - \sigma_i^2\left(\mu_{22} + \mu_{33} - \sigma_i^2\right) - \mu_{23}^2\right] \Big/ D_i \; ; i = 1, 2, 3 \tag{11}$$

$$m_i = \left[\mu_{23}\mu_{13} - \mu_{12}\mu_{33} + \sigma_i^2\mu_{12}\right] \Big/ D_i \; ; i = 1, 2, 3 \tag{12}$$

$$n_i = \left[\mu_{12}\mu_{23} - \mu_{13}\mu_{22} + \sigma_i^2\mu_{13}\right] \Big/ D_i \; ; i = 1, 2, 3 \tag{13}$$

where

$$\begin{aligned} D_i^2 = {} & \left(\mu_{22}\mu_{33} - \mu_{23}^2\right)^2 + \left(\mu_{23}\mu_{13} - \mu_{12}\mu_{33}\right)^2 + \left(\mu_{12}\mu_{23} - \mu_{13}\mu_{22}\right)^2 \\ & + 2\left[\left(\mu_{22} + \mu_{33}\right)\left(\mu_{23}^2 - \mu_{22}\mu_{33}\right) + \mu_{12}\left(\mu_{23}\mu_{13} - \mu_{12}\mu_{33}\right) + \mu_{13}\left(\mu_{12}\mu_{23} - \mu_{13}\mu_{22}\right)\right]\sigma_i^2 \\ & + \left(\mu_{33}^2 + 4\mu_{22}\mu_{33} + \mu_{22}^2 - 2\mu_{23}^2 + \mu_{12}^2 + \mu_{13}^2\right)\sigma_i^4 - 2\left(\mu_{22} + \mu_{33}\right)\sigma_i^6 + \sigma_i^8. \end{aligned}$$

• *Solar motion elements*
The Solar motion can be defined as the absolute value of the Sun's velocity $S_\odot$ (although it is not a vector) relative to the objects under consideration, i.e.

$$S_\odot = \sqrt{\overline{U}^2 + \overline{V}^2 + \overline{W}^2}(km/s). \tag{14}$$

The Galactic longitude l_A and Galactic latitude b_A of the Solar apex is

$$l_A = \tan^{-1}(-\overline{V}/\overline{U}), \tag{15}$$

$$b_A = \sin^{-1}(-\overline{W}/S_\odot). \tag{16}$$

These three parameters may be considered as the elements of Solar motion with respect to these open clusters groups under consideration.

Based on the computational algorithm presented above, a *Mathematica* routine has been developed to compute the kinematical parameters of these five groups. Fig. 2 shows the distribution of the space velocities of 56 open clusters. The kinematical parameters of these five groups as well as the elements of Solar motion are listed in Table 3 in the following format:

Row 1: The Frequencies.

Rows 2, 3, and 4: The average components of space velocities whose center is the Sun.

Rows 5, 6, and 7: The average components of space velocities due to Galactic coordinates.

Row 8: Total space velocity (i.e. $\sqrt{\overline{U}^2 + \overline{V}^2 + \overline{W}^2}$.

Rows 9, 10 and 11: The eigenvalues.
Rows 12, 13 and 14: The dispersion velocity.
Row 15: Total dispersion velocity (σ_o).
Row 16: The dispersion ratio (σ_2/σ_1).
Rows 17, 18, 19, 20, 21, 22, 23, 24, and 25: The direction cosines parameters.
Rows 26, 27, and 28: The elements of the Solar motion.

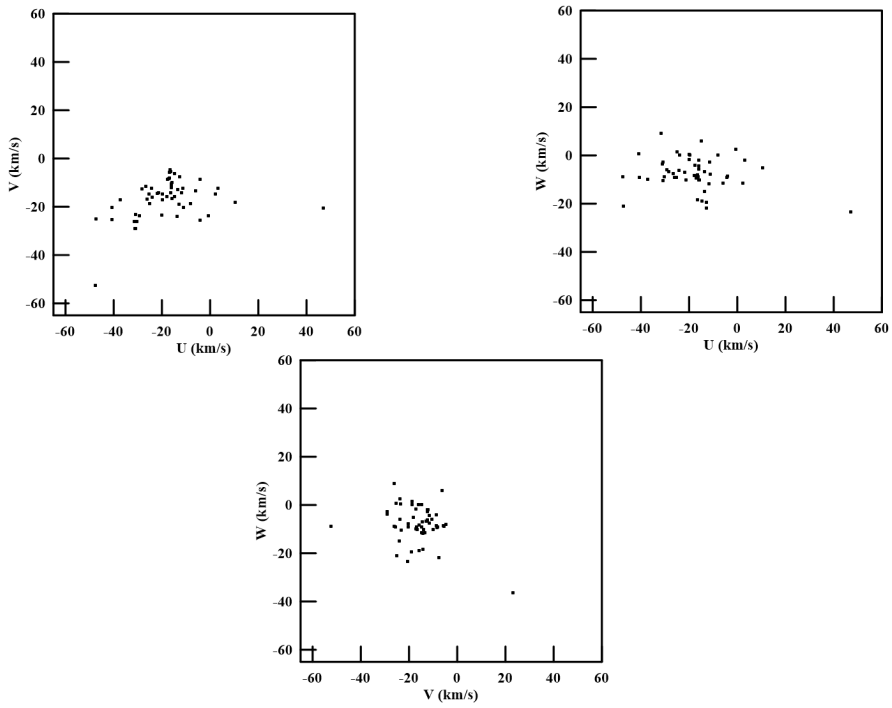

Fig. 2. The velocity distribution of 56 open clusters under consideration, showing the V *vs.* U in the left upper panel, the W *vs.* U in the right upper panel, and the W *vs.* V in the lower panel

3. Luminosity and mass functions analysis

Let us now turn to the problem of determining the luminosity function $\phi(M_J)$, which is among the most important tools to analyze the composition and evolution of stellar systems, especially in studies of open star clusters (Elsanhoury et al., 2011).

The integrated luminosity function LF $\phi(M_J)$ of open clusters can be used to obtain information on the frequency distribution of clusters of various luminosities and to estimate the total number of clusters in the vicinity

Table 3. The velocity ellipsoid parameters VEPs of five open clusters groups and their elements of the Solar motion

Parameters	Group I	Group II	Group III	Group IV	Group V
Frequencies	13	19	9	12	3
V_x, km/s	-1.340 ± 0.040	2.928 ± 0.711	-2.101 ± 0.449	-0.130 ± 0.005	-7.766 ± 2.787
V_y, km/s	18.632 ± 4.316	18.088 ± 4.253	31.981 ± 5.655	26.071 ± 5.106	32.722 ± 5.720
V_z, km/s	-8.737 ± 2.956	-5.512 ± 2.348	-7.596 ± 2.756	-8.715 ± 2.952	-12.488 ± 3.534
$\overline{U}$, km/s	-11.933 ± 3.454	-13.248 ± 3.640	-24.091 ± 4.908	-18.495 ± 4.301	-22.065 ± 4.697
$\overline{V}$, km/s	-15.557 ± 3.944	-10.822 ± 3.290	-21.046 ± 4.588	-18.286 ± 4.276	-27.800 ± 5.273
$\overline{W}$, km/s	-6.393 ± 2.528	-8.574 ± 2.928	-7.846 ± 2.801	-8.903 ± 2.984	-5.227 ± 2.286
Spa. Vel., km/s	20.622 ± 4.542	19.134 ± 4.374	25.748 ± 5.074	27.490 ± 5.243	35.875 ±5.990
λ_1, km/s	577.661 ± 24.035	718.271 ± 26.801	1287.46 ± 35.881	841.029 ± 29.000	940.294 ± 30.664
λ_2, km/s	231.349 ± 15.210	157.537 ± 12.551	78.428 ± 8.856	95.817 ± 9.789	86.938 ± 9.324
λ_3, km/s	40.054 ± 6.329	20.580 ± 4.537	56.323 ± 7.505	28.780 ± 5.365	0.152 ± 0.050
σ_1, km/s	24.035 ± 4.903	26.801 ± 5.177	35.881 ± 5.990	29.001 ± 5.385	30.664 ± 5.538
σ_2, km/s	15.210 ± 3.900	12.551 ± 3.543	8.856 ± 2.976	9.789 ± 3.129	9.324 ± 3.054
σ_3, km/s	6.329 ± 2.516	4.536 ± 0.130	7.505 ± 1.740	5.365 ± 0.316	0.390 ± 0.005
σ_o, km/s	29.155 ± 5.400	29.940 ± 5.472	37.712 ± 6.141	31.075 ± 5.575	32.053 ± 5.662
$\sigma_2/\sigma 1$	0.64 ± 0.05	0.47 ± 0.04	0.25 ± 0.01	0.34 ± 0.02	0.31 ± 0.01
l_1, degrees	0.906	0.872	0.767	0.742	0.686
l_2, degrees	-0.412	-0.171	-0.642	-0.441	-0.684
l_3, degrees	0.104	0.460	0.026	0.506	0.248
m_1, degrees	0.414	0.490	0.620	0.615	0.721
m_2, degrees	0.806	0.254	0.751	0.142	0.589
m_3, degrees	-0.422	-0.834	0.227	-0.777	-0.366
n_1, degrees	0.091	0.026	0.166	0.271	0.104
n_2, degrees	0.425	0.952	0.158	0.886	0.430
n_3, degrees	0.901	0.305	-0.973	0.376	0.897
l_A, degrees	-52.511	-39.245	-41.141	-44.675	-51.561
b_A, degrees	18.060	26.621	13.780	18.897	8.378
$S_\odot$, km/s	20.623 ± 4.54	19.135 ± 4.37	32.938 ± 5.74	27.490 ± 5.24	35.874 ± 6.00

of the Sun. This function is first determined by Collinder (1931). Subsequently, it was constructed by Kopylov & Krymsk (1951) using data of 300 clusters situated within a sphere of 2 kpc in radius. He also showed that the luminosity of clusters is primarily governed by the luminosities of stars of the earliest spectral types belonging to the clusters (Starikova 1965).

Table 4. The double frequency table DFT of our 56 open clusters sample

Distance	98.717 - 310.078	310.078 - 521.439	521.439 - 732.800	732.800 - 944.161	944.161 - 1155.522
-7.890 - -6.869		1			
-6.869 - -5.848		1		1	1
-5.848 - -4.827		1	1	1	3
-4.827 - -3.809		1	3	2	1
-3.806 - -2.785	2	2	1	3	2
-2.785 - -1.764	4	8	3	1	3
-1.764 - -0.743		3	1	3	
-0.743 - 0.278	3				

In what follows of our analysis, $\phi(M_J)$ was determined using the classical method of van Rhijn (1965), into which LF is defined as the number of objects in certain magnitude interval per unit volume (zone). This volume is large enough to contain a statistically useful sample of objects while still small enough that interstellar absorption can be neglected within it. Inside this sphere, the volume and magnitude elements were determined by dividing the whole volume into circular zones around the Sun. A double frequency table DFT (distribution into equal magnitudes and distance intervals) was constructed into which a number of clusters in each zone (shell) corresponding to each magnitude interval (min. mag = -7.890 and max. mag = -0.252) is established as shown in Table 4. We can determine the LF, i.e. the total number of clusters that fall in the magnitude interval

corresponding to specific volume interval (van Rhijn 1965) as listed in Table 5. Fig. 3 presents the LF of these open clusters [M_J *vs. Log* $\phi(M_J)$] like Elsanhoury et al. (2011) and Elsanhoury (2013). This luminosity function is often referred to as the van Rhijn luminosity function in recognition to van Rhijn's pioneering efforts in its determination.

Table 5. Our luminosity function LF determination of 56 open clusters

M_J	$\phi(M_J)$	*Log* $\phi(M_J)$
-7.380	2.088×10^{-9}	-8.681
-6.359	2.943×10^{-9}	-8.531
-5.338	4.539×10^{-9}	-8.343
-4.317	6.251×10^{-9}	-8.204
-3.300	2.355×10^{-8}	-7.628
-2.275	5.344×10^{-8}	-7.272
-1.254	8.759×10^{-8}	-8.058
-0.233	2.431×10^{-8}	-7.614

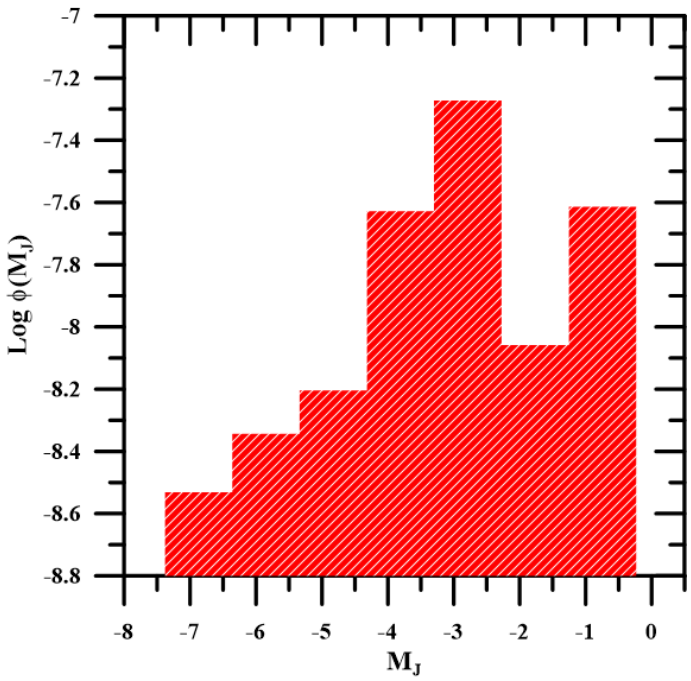

Fig. 3. The luminosity function LF [M_J *vs. Log* $\phi(M_J)$] of 56 open clusters

The present-day mass function PDMF $\phi_{ms}(Log\ M)$ is defined as the number of objects per unit logarithmic mass interval per square parsec in the Solar neighborhood (Miller & Scalo 1979). The PDMF is related to the LF $\phi_{ms}(M_J)$ by:

$$\phi_{ms}(Log\ M) = \phi(M_J)|\frac{dM_V}{d\ Log\ M}|2H(M_J)f_{ms}(M_J). \qquad (17)$$

Table 6. Our initial mass function IMF determination of 56 open clusters

M_J	$Log\ (M/M_\odot)$	$Log\ \xi(Log\ (M/M_\odot))$
-7.380	1.813	-6.516
-6.359	1.644	-5.442
-5.338	1.479	-4.469
-4.317	1.318	-3.593
-3.300	1.162	-2.810
-2.275	1.010	-2.106
-1.254	0.862	-1.484
-0.233	0.719	-0.938

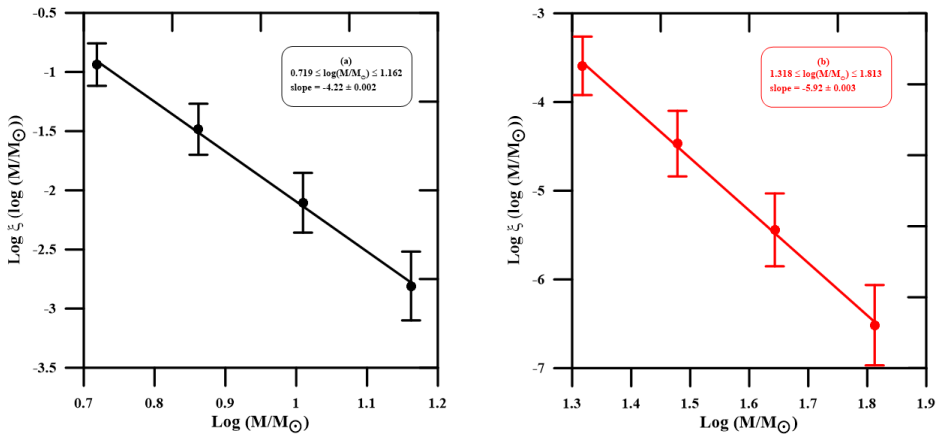

Fig. 4. The initial mass function IMF [$Log\ (M/M_\odot)$ *vs.* $Log\ \xi(Log\ (M/M_\odot))$] of 56 open clusters with error bars, showing slopes of *left* panel (a) and *right* panel (b) about -4.22 ± 0.002 and -5.92 ± 0.003 respectively

where $dM_J/d\ Log\ M$ is the slope of the (absolute magnitude, mass) - relation and converts the LF to MF. The term $2H(M_J)$ is the result of integrating LF perpendicular to the plane of the Galaxy, assuming an exponential distribution with scale height $H(M_J)$. The factor $f_{ms}(M_J)$ gives the fraction of objects at a given magnitude (Miller & Scalo 1979).

By referring to Equation (17), we aimed to study the IMF of these 56 open clusters under investigation, Table 6 gives the IMF of the objects under consideration, while Fig. 4 presents the IMF [$Log\ (M/M_{\odot})$ *vs. Log* $\xi(Log\ (M/M_{\odot}))$], the slope of the left panel is about -4.22 $\pm$ 0.002 for $0.719 \leq Log\ (M/M_{\odot}) \leq 1.162$ seems like Chabrier (2003) (i.e. $\sim$ -3.53 with $0.54 \leq Log\ (M/M_{\odot}) \leq 1.26$) while the slope of the right panel is about -5.92 $\pm$ 0.003 for $1.318 \leq Log\ (M/M_{\odot}) \leq 1.813$ which is not in agreement with Chabrier (2003) (i.e. $\sim$ -2.11 with $1.26 \leq Log\ (M/M_{\odot}) \leq 1.80$).

4. Results and discusion

First, we focused on the self-comparison between these five groups. The dispersion velocities $(\sigma_1, \sigma_2, \sigma_3)$ are comparable for these sets, while the Solar velocity $S_{\odot}$ is quite different.

Another comparison possible with the present results is that between these sets with different distances ($\leq$ 1 kpc); results are significant for the ratio of (σ_2/σ_1) which reflects the differences in the initial structure (ages and chemical compositions). Important quantities in stellar and/or groups are the Oort constants A and B. The relation between these constants and the ratio (σ_2/σ_1) is given like $(\sigma_2/\sigma_1)^2 = -B/(A-B)$, where the constants are characterized by the local relation properties of our Galaxy. The list of values of these constants are given in Table 7 according to Olling & Merrifield (1998), in which the first and second columns give the Oort constants A and B respectively, while the third column presents the ratio (σ_2/σ_1) calculated with that Oort constants.

For the first group ($98.717 \leq r \leq 310.078$ pc), we notice that for our calculations $(\sigma_2/\sigma_1) = 0.64$ is in the range of 0.65-0.74 presented in Table 7. For distances greater than 310.078 pc, we notice that these values do not coincide with a range in that table. We can reflect that due to distances, the formation mechanism that is affected by various physical conditions, such as metallicity and opacity (Silk,1979 and Yoshii & Saio, 1985), turbulent motion (Hunter & Flecker, 1982 and Flecker, 1982), hierarchical fragmentation (Larson, 1973 and Zinnecker, 1984), and the interaction of fragments (Bastien, 1981 and Silk & Takahashi, 1979).

Table 7. The Oort's constants (A, B) and dispersion ratio (σ_2/σ_1)

$A(km\ s^{-1}\ kpc^{-1})$	$B(km\ s^{-1}\ kpc^{-1})$	(σ_2/σ_1)	Author
14.5 $\pm$ 1.3	-12 $\pm$ 2.8	0.65	Kerr & Lynden-Bell (1986)
12.6	-13.2	0.71	Brand & Blitz (1993)
14.8 $\pm$ 0.8	-12.4 $\pm$ 0.6	0.67	Feast & Whitelock (1997)
11.3 $\pm$ 1.1	-13.9 $\pm$ 0.9	0.74	Olling & Merrifield (1998)

According to the LF behavior as shown in Fig. 2, we can infer that; the bright clusters are visible at greater distances, while the faint clusters are only visible when nearby, on the other hand, the massive bright objects

seem to be centrally concentrated more than the low-mass and fainter ones (Montgomery et al., 1993). Moreover, the steep slope of the IMF indicates that the number of low-mass objects is greater than the high-mass ones like drawn in Fig. 4.

Recently Bobylov & Bajkova (2019) used the same catalog of Gaia DR2 to study the kinematics of the Galaxy for the sample of 326 young open clusters with ($Log\ t < 8\ yr$), they concluded that the dependence of dispersion velocity σ_o shows growth with increasing stellar age (disk heating).

Conclusion

In the present work for a list of 56 open clusters within 1 kpc with known radial velocities and magnitudes, the velocity ellipsoid parameters VEPs (e.g. space velocity, dispersion velocity, direction cosines parameters, and elements of Solar motion) are determined. Also, the luminosity and mass functions based on this sample are presented. The following points may draw the reached conclusions:

• Dependence on the distances, we classify 56 open clusters according to Sturges's rule into five groups (classes).

• For these classes, we determined VEPs and then computed the dispersion ratio (σ_2/σ_1).

• For open clusters with $98.717 \leq r \leq 310.078$ pc, the ratio (σ_2/σ_1) is in good agreement with Olling & Merrifield (1998).

• For open clusters whose distances $r > 310.078$ pc, the ratio of (σ_2/σ_1) is not in the range of Olling & Merrifield (1998), this may be due to distances and/or formation mechanisms.

• We have determined their luminosity function dependence on their absolute magnitudes M_J, as well as their mass functions by the mass luminosity relation.

Acknowledgments

The author would like to thank the referee for very useful and important suggestions that improved this article.

This work presents results from the European Space Agency (ESA) space mission Gaia. Gaia data are being processed by the Gaia Data Processing and Analysis Consortium (DPAC). Funding for the DPAC is provided by national institutions, in particular, the institutions participating in the Gaia Multi-Lateral Agreement (MLA). The Gaia mission website is https://www.cosmos.esa.int/gaia. The Gaia archive website is https://archives.esac.esa.int/gaia.

References

Bastien P., 1981, *Astron. Astrophys., 93, 160*
Bobylev V. V. and Bajkova A. T., 2019, *Astron. L., 45, No. 3, 109*
Brand J. and Blitz L., 1993, *Astron. Astrophys., 275, 67*

Cantat-Gaudin T., Jordi C., Vallenari A., Bragaglia A., Balaguer-Núñez L., Soubiran C. , Bossini D., Moitinho A., Castro-Ginard A., Krone-Martins A., Casamiquela L., Sordo R., and Carrera R., 2018, *Astron. Astrophys., 618, A93*
Chabrier G., 2003, *Publ. Astron. Soc. Pac., 115, 763*
Collinder P., 1931, *Ann. Observ. Lund, No. 2*
Dehnen W. and Binney J. J., 1998, *Mon. Not. R. Astron. Soc., 298, 387*
Elsanhoury W. H., Hamdy M. A., Nouh M. I., Saad A. S., and Saad S. M., 2011,*ISRN Astron. Astrophys., 2011, ID 127030*
Elsanhoury W. H., 2013, *Romanian Astron. J., 23, No. 1, 15*
Elsanhoury W. H., Sharaf M. A., Nouh M. I., and Saad A. S., 2013, *Open Astron. J., 6, 1*
Elsanhoury W. H., Nouh M. I., and Abdel-Rahman H. H., 2015, *Rev. Mex. Astron. Astrofis, 51, 197*
Elsanhoury W. H., Haroon A. A., Chupina N. V., Vereshchagin S. V., Sariya Devesh P., Yadav R. K. S., and Jiang I.-G., 2016,*New Astron., 49, 32*
Feast M. and Whitelock P., 1997, *Mon. Not. R. Astron. Soc., 291, 683*
Flecker R. C., 1982, *Mon. Not. R. Astron. Soc., 201, 551*
Freedman D. and Diaconis P., 1981, *On this histogram as a density estimator: L2 theory. Zeit. Wahr. ver. Geb., 57, 453*
Hogg D. W., Blanton S. T., Roweis S. T., and Johnson K. V., 2005,*Astrophys. J., 629, 268*
Hunter J. H. and Flecker R. C., 1982, *Astrophys. J., 256, 505*
Joshi Y. C., Dambis A. K., Pandey A. K., and Joshi S., 2016,*Astron. Astrophys., 593, A116*
Kharchenko N. V., Piskunov A. E., Roeser et al., 2013, *Astron. Astrophys., 558, A53*
Kharchenko N. V., Piskunov A. E., Schilbach E., Roeser S., and Scholz R.-D., 2016,*Astron. Astrophys. 585, 101*
Kerr F. J. and Lynden-Bell D., 1986, *Mon. Not. R. Astron. Soc., 221, 1023*
Kopylov, I. M. and Izv Krymsk, 1952, *astrofiz. Observ., 8, 122* y
Larson R. B., 1973, *Mon. Not. R. Astron. Soc., 161, 133*
Liu J. -C., Zhu Z., and Hu B., 2011, *Astron. Astrophys., 536, A102*
Miller G. E. and Scalo J. N., 1979, *Astrophys. J. Supp. Ser., 41, 513*
Montgomery K. A., Marschall L. A., Janes K. A., 1993, *Astron. J., 106, 181*
Olling R. P. and Merrifield M. R., 1998, *Mon. Not. R. Astron. Soc., 297, 943*
Silk J., 1979, *Astrophys. J., 214, 718*
Silk J. and Takahashi T., 1979, *Astrophys. J., 229, 242*
Smart W. M., 1958, *Combination of observations, Cambridge University Press, London*
Starikova G. A., 1965, *Soviet Astrono., vol. 8, 4, 598*
van Rhijn P. J., 1965, *Pub. Kapteyn Astron. Lab. Groningen, No. 47*
Yoshii Y. and Saio H., 1985, *Astrophys. J., 295, 521*
Zinnecker H., 1984, *Mon. Not. R. Astron. Soc., 210, 43*